LABORATORI NAZIONALI DI FRASCATI
SIS – Pubblicazioni

LNF–97/041 (P)
27 Novembre 1997

Characterization of Local Chemistry and Disorder in Synthetic and Natural α-Al_2O_3 Materials by X-ray Absorption Near Edge Structure Spectroscopy

A. Mottana[1,3], T. Murata[2], A. Marcelli[3], G. Della Ventura[4, 3], G. Cibin[3], Z. Wu[5], R. Tessadri[6]

[1] Universita' di Roma Tre, Dip. di Scienze Geologiche, Largo San Leonardo Murialdo 1, I-00146 Roma RM, Italy
[2] Kyoto University of Education, Department of Physics, 1 Fujinomori-cho, Fukakusa, Fushimi-ku, Kyoto 612, Japan
[3] Istituto Nazionale di Fisica Nucleare, Laboratori Nazionali di Frascati, Via Fermi 40, I-00044 Frascati RM, Italy
[4] Univ. di Roma Tre, Dipartimento di Scienze Geologiche, Largo San Leonardo Murialdo 1, I-00146 Roma RM, Italy
[5] Commissariat à l'Energie Atomique, DSM/DRECAM/SRSIM, Bat. 462, CE Saclay, 91191 Gif-sur-Yvette Cedex, France
[6] Universität Innsbruck, Institut für Mineralogie und Petrographie, Innrain 62, A-6020 Innsbruck, Austria

Abstract

X-ray absorption fine spectra at the Al K-edge were measured experimentally on and calculated theoretically *via* the multiple-scattering formalism for a chemically pure and physically perfect synthetic α-Al_2O_3 (α-alumina), a natural "ruby/sapphire" (corundum) and a series of artificial "corundums" produced for technical purposes and used as geochemical standards. The Al K-edge spectra differ despite of the identical coordination (short-range arrangement) assumed by O around Al, and vary slightly in relation to the slightly different chemistries of the materials (substitutional defects) as well as on account of the location taken by foreign atoms in the structural lattices (positional defects). A quantitative treatment of the observed changes is made in terms of short-range modification of the coordination polyhedron and of medium- to long-range modifications in the overall structure; both of them induced by substitutions. In some technical "corundums", the impurities of admixed "β-alumina", where Al is both in four- and six-fold coordination, produce another small but detectable effect on Al K-edges. Therefore, XAFS spectroscopy proves its potentials for both measuring a light element such as Al, and detecting minor coordination changes and substitutions (ca. 1~3 wt.% as oxide) of the absorber by dilute other atoms, at least under favorable conditions as those occurring in this system are.

PACS.: 78.70.Dm,81.40.P,61.72.-y
Key words: X-Ray Absorption; Abrasion materials; Defects and impurities in crystals; alumina.

Submitted to *Journal of Applied Crystallography*

1 – INTRODUCTION

Aluminum oxide is one of the most important metal oxides for technical applications, and by far the most important single substance used in the abrasive industry. Many studies have been dedicated to it including, recently, some dealing with the fundamentals of its structure and electronic behavior. Indeed, the physical properties of all materials depend on both the arrangement of their constituting atoms, and the electronic properties of these. This holds particularly true for simple compounds such as Al_2O_3, where variations in the properties away from the values determined on chemically and structurally "ideal" samples can only depend upon subtle atomic changes, which generate what is appropriately known as a defect. There are two types of defects: (i) *substitutional*, in the case of foreign atoms substituting for Al, and (ii) *positional*, in the case of Al (or any other atom) being displaced from the expected lattice site, if not entirely missing (ii^a: *omission*) or added (ii^b: *addition*).

Theoretical and experimental studies on Al_2O_3 date back to long ago and involve a variety of different methods (e.g., Tossel 1975; Balzarotti & Bianconi 1976; Brytov et al. 1979; Batra 1981; Ciraci & Batra 1983; Causa' et al. 1987; McKeown 1989; Kirfel & Eichhorn 1990; Blonski & Garofalini 1993; Wong et al. 1994; Ildefonse et al. 1994; Li et al. 1995, 1996; Cabaret et al. 1996). Previous works disclosed the existence of several metastable phases (β, β", γ, η, etc.) in addition to describing in detail the stable α-phase (corundum); yet all metastable phases were found to be of technical importance.

Most early experimental works were done on one sample only, usually a synthetic one. By contrast, in the present paper we examine the electronic properties of Al in a series of synthetic Al_2O_3 materials of variable but known composition especially prepared to be used as standards (Tessadri 1996). To understand their behavior, we also studied for comparison a pure synthetic α-Al_2O_3 and a natural corundum. The method we use is X-ray Absorption Near-Edge Spectroscopy (XANES) at the Al K-edge.

Our study aims at:

(a) Showing the potential of XANES to solve the local crystal-chemistry and describe the site symmetry etc. (cf. Bianconi 1988) even for an element that was considered inaccessible till few years ago because its absorption K-edge lies in the range of soft X-rays;

(b) Assessing the potential and reliability of XANES when applied to samples of slightly variable but essentially the same composition i.e., where the absorber is always the same but minor amounts of it are being substituted by other atoms;

(c) Verifying in simple systems the sensitivity of XANES as a technique for determining the extent of local order probed by the photoelectrons, as we have already demonstrated in garnets (Wu et al. 1996a) and feldspars (Wu et al. 1997).

2 – MATERIALS

Five synthetic Al_2O_3 materials were prepared at Innsbruck University in cooperation with Treibacher Schleifmittel and Tyrolit-Schleifmittelwerke, Austria (Table I). In the chemical sense, they are almost pure alumina "bulk materials" since they all consist of 97~99 wt.% Al_2O_3; however, physically speaking, they never are pure homogeneous α-phases (i.e., corundums), because they contain impurities in the form of admixed phases quantitatively revealed by X-ray diffraction (XRD).

TABLE I – Major, minor, and trace components (ppm, both oxides and elements) of synthetic Al_2O_3 (COR 1 → COR 5) and natural "ruby/sapphire" corundum (COR 6).

	COR 1	**COR 2**	**COR 3**	**COR 4**	**COR 5**	**COR 6**
Cao	209	184	168	319	347	1600
Cr_2O_3	74	2270	1260	148	177	900
Cu	14	12	3	5	1	3
Fe_2O_3	287	482	616	1480	1720	9200
MgO	49	20	33	749	2100	400
MnO	12	9	17	143	150	16
Na_2O	3410	1540	1200	372	175	200
Nb	3	4	2	3	3	20
NiO	<5	<5	<5	<5	<5	20
Sc	1	1	1	35	32	1
SiO_2	175	77	105	2920	4370	3700
Sr	10	5	6	20	36	12
TiO_2	22	<5	2290	16200	25000	12700
V_2O_5	10	3	18	33	48	34
Y_2O_3	36	3	1	67	65	170
Zn	19	12	14	4	3	4
ZrO_2	1	1	1	1100	1100	900

COR 1 (commercially distributed as "precious white corundum") contains ˜10 vol.% admixture of phase $Na_{1-x}Al_{11}O_{17+x}$ (the so-called "β–alumina", actually a sodium aluminate with the defect spinel structure; cf. Edström et al. 1991; Rocca et al. 1996) owing to the synthesis process for which NaOH is used as flux. COR 2 ("precious pink") and COR 3 ("precious pink special") also contain minor "β–alumina" (˜3~5 vol.%) and some Cr_2O_3, both being due to the synthesis process and the latter component believed to be a chemical impurity dissolved in the admixed "β-alumina". These samples constitute a group, which is homogeneous not only for all these samples contain physical impurities of "β–alumina", but for their bulk chemistries, all rather pure: notwithstanding their high Na_2O contents, the total amounts of impurities measured in them are barely $0.4\sim0.6\times10^4$ ppm (Table I: Al_2O_3 ≥99 wt.%): COR 1, in particular, is the purest sample of the whole set.

The second group of artificial samples comprises COR 4 ("semi-precious") and COR 5 ("normal") "corundums". They are rather impure, both chemically (Table I: Al_2O_3 ≤97 wt.%; measured impurities $2.3\sim3.5\times10^4$ ppm), owing to the fact that they contain various components all believed to be derived from agents used during the synthesis process, and physically, since XRD gives evidence that most of these elements occur as admixtures i.e, as complex titanates, spinels, ferro-silicium etc. However, XRD at this level of resolution cannot give a straightforward answer to the possibility that at least some of the detected chemical impurities are dissolved in corundum, nor that both physical and chemical impurities may be present together.

COR 6 ("ruby/sapphire") is a finely milled mix of natural red and blue corundum crystals from Tanzania, originally 1 to 5 cm in diameter, and was especially prepared to be used as a geochemical standard (Tessadri 1996). It is chemically rather impure (Table I: Al_2O_3 ≈97 wt.%; determined impurities 3.0×10^4 ppm) not only because it contains a great number of small inclusions of rutile, Al-hydroxides, etc., but also because of its structural substitutions, as warranted by its colors.

However, the unit-cell parameters (Table II) indicate that most chemical impurities do not enter the corundum lattice; as a matter of fact COR 6, on the basis of its volume, is purer than COR 4 and COR 5, almost as pure as COR 1-2-3.

The pure-in-composition (100 wt.% Al_2O_3), synthetic α-alumina used as reference material was obtained by firing at 1400°C in air an aluminum hydroxide gel (prepared from suprapure Al foil according to the method of Hamilton & Henderson 1968).

3 – STRUCTURAL INFORMATION

Corundum, or *α-alumina*, Al_2O_3-$R\bar{3}c$, is trigonal with a_R = 0.5128 nm, α = 55.18°, Z_R = 1 (alternatively: a_H = 0.47589 nm, c_H = 1.29911 nm, Z_H = 6, when in the hexagonal setting; cf. Newnham & deHaan 1961). Ideally, it has a honeycomb-like structure where Al occupies one third of the equivalent octahedral voids of a hexagonal closest packing formed by O, thus attaining the most symmetrical distribution for spheres in the 2:3 ratio. In fact, in the real structure (Fig. 1) the Al cation, with point symmetry 3, is at the center of a slightly distorted octahedron of O anions symmetrically distributed over two alternating positions O1 and O1'. Therefore, the Al-O bonds are alternatively three long (Al-O1 = 0.1969 nm) and three short (Al-O1' = 0.1856 nm), with the 12 octahedral angles also symmetrical: 6 × O1-Al-O1 = 86.4°, 3× O1-Al-O1' = 79.7°, and 3× O1-Al-O1' = 101.1°; quadratic elongation is 1.0200 and angle variance 66.6. All Al-O bonds are highly polar in character (Sousa et al. 1993). There are natural corundums so close to endmember composition as to be practically identical to a pure synthetic sample: this variety is known as "leucosapphire", colorless, translucent or even transparent. As a result of the high packing index (0.77) and isodesmic bond distribution, such corundums have bulk properties next to being extreme (density 3.986 $g\cdot cm^3$, melting point 2323 K, Mohs' hardness 9); they display no cleavage, but a uneven conchoidal fracture, and their refraction indices are high (n_O 1.768, n_E 1.760) so that luster is close to subadamantine.

Synthetic α-Al_2O_3 and natural corundums acquire color when defects are present (Schmetzer & Bank 1981). Most important are the simple chemical substitutions for Al, which lead to "ruby", red (Al <-> Cr), and "sapphire", blue (Al <-> Fe). Other less common varieties arising from complex chemical substitutions are "padparadschah", orange, "oriental emerald", green, "oriental topaz", yellow, etc. A variety arising from physical defects (admixture of rutile needle) is “asteria”. "Emery" is the common name for finely granular corundum used as abrasive, normally gray or brown as a result of several different impurities and defects.

Aluminas used for emery have different abrasive properties, not only as a result of their impurities, if natural, but also for there are intrinsic differences among different samples, probably as a result of their changing bond hardness with the amount of defects present. This is supported by evidence deduced from synthetic α-Al_2O_3, as most corundum-based abrasives are no longer natural, but artificially made to meet special industrial requirements.

TABLE II – Lattice constants of COR 1 to COR 6.

	COR 1	**COR 2**	**COR 3**	**COR 4**	**COR 5**	**COR 6**
a (Å)	4.7577	4.7582	4.7581	4.7605	4.7624	4.7591
c (Å)	12.9871	12.9883	12.9883	12.9941	12.9993	12.9909
V (Å^3)	254.59	254.66	254.65	255.02	255.33	254.81

4 – EXPERIMENTAL METHODS

4.1 – XAS spectroscopy

The XAS spectra were collected at UVSOR, the synchrotron radiation source of Institute of Molecular Science (IMS) at Okazaki, Japan, a 750 MeV electron storage ring operating at 200 mA current with a lifetime of about 4 h (Watanabe 1991).

The soft X-ray beamline BL7A derives SR by a superconducting wiggler under an acceptance angle of 1 mrad in the horizontal plane and of 0.15 mrad in the vertical plane, yielding photons in the energy range 800-4000 eV. The beamline is equipped with a double-crystal monochromator which may accomodate several crystals. We used either (400) YB_{66} or $(10\bar{1}0)$ quartz (Murata et al. 1992), both of which scan the Al K-edge by angle steps as small as $0.01^{o}\theta$; however, the reported results concern only YB_{66}. From the width of the Al K-edge white-line we believe that resolution is certainly better than 1.27 eV; our analysis suggests it to be around 1.0 eV, in agreement with measurements on the rocking curve (Kinoshita et al. 1997). The sample is spread as a very fine film on a piece of graphite tape, which is adhesive on both sides. The other side of the tape is sticked onto the first photocatode of an electron multiplier, which measures the total yield of the photoelectrons emitted from the sample by the x-ray excitation as its output current. The entire monochromator plus sample system is held in a vacuum chamber at $1\mathbf{x}10^{-7}$ torr.

All experimental spectra were recorded at least twice at different times, externally calibrated against a standard Al foil (1559.8 eV), and found to be consistent. The energy value of each feature was measured by fitting a lorentzian line, with errors always well below 0.1 eV within each spectrum and with $2\sigma \approx 0.1$ eV among different spectra. The heights of each individual feature relative to the related white-line appear to be reproducible to within ±5%, but were not tabulated owing to unresolved problems on how to establish a correct quantitative model of evaluation.

4.2 – MS calculation

Theoretical spectra have been calculated by the XANES CONTINUUM code (Natoli et al. 1990), which is based on the one-electron multiple-scattering (MS) theory (Lee & Pendry 1975), and was implemented both computationally and theoretically so as to prove successful in a variety of physical systems (e.g. Tyson et al. 1992; Mottana et al. 1996, 1997; Wu et al. 1996a, 1996b, 1997).

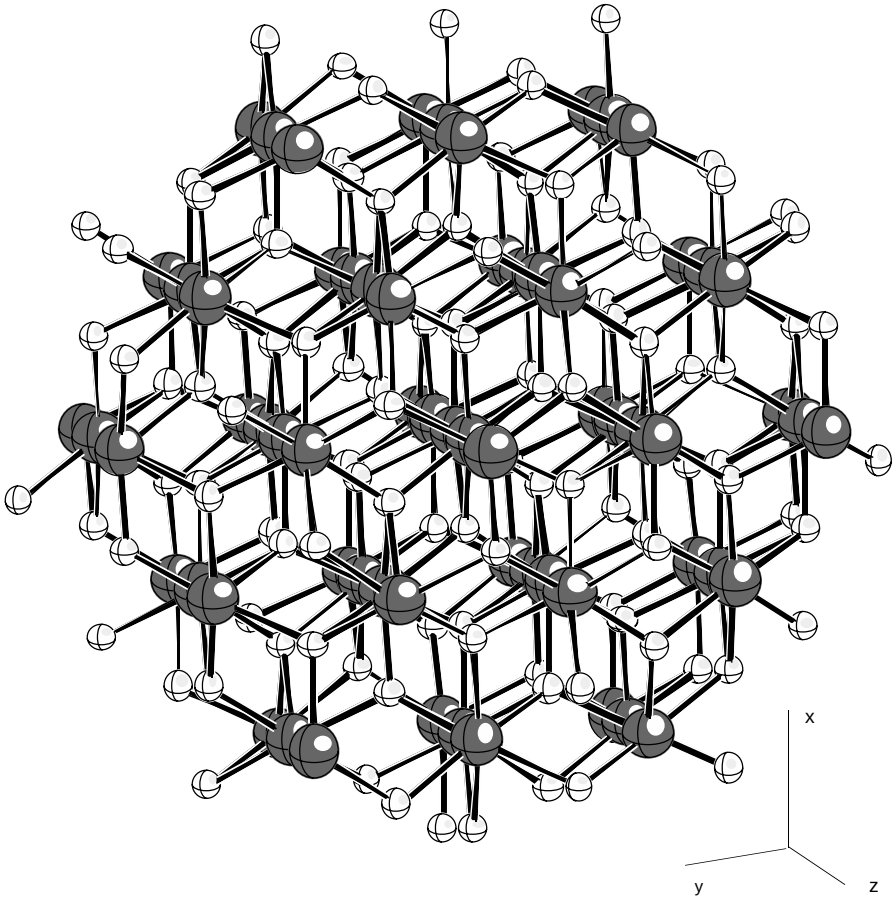

FIG. 1 – The structure of α-Al_2O_3 (corundum) for a cluster extending to 1.52 nm from the Al absorber and including 143 (Al + O) atoms.

Full details on this scheme have been given elsewhere (cf. Tyson et al. 1992; Wu et al. 1996a) and only little information needs to be added here. The total potentials of clusters were constructed in the muffin-tin approximation according to Mattheiss' (1964) prescription, i.e. by superimposition of neutral atomic charge densities using Clementi and Roetti's (1974) basis data set. Muffin tin radii were chosen according the criterion of Norman (1974), and a 10% overlap between contiguous spheres was allowed to simulate the ionic bond.

The energy-independent Xα type of exchange (Slater 1979) was used instead of the Hedin-Lundqvist (1971) real one, since the latter, although fitting well the IMS region of the spectra, appears to give calculated features in the FMS region that are too contracted relative to the experimental ones. Calculations were routinely made at steps 0.05 Ry (i.e., 0.68 eV), but in FMS region, where the step width was reduced to 0.025 Ry. Spectra are plotted without accounting for any form of broadening or smoothing. In calculating, we followed the same line of approach as Cabaret et al. (1996) did, but only up to a cluster containing 143 atoms i.e., up to 1.52 nm away from the central absorbing Al atom; as a matter of fact, we found that a 90-atom cluster qualitatively fits the experimental data best.

4 – EXPERIMENTAL RESULTS

The pure α-alumina Al K-edge X-ray absorption spectrum (Fig. 2a) consists of a sharp white-line at 1568.3 eV (A, with FWHM 1.28 eV) which is preceded by a very weak, shoulder-like pre-peak at 1565.8 eV (A') and is followed by a second, fairly strong but not as sharp feature at 1572.2 eV (B); this has a shoulder (C) on its higher energy side (1574.1 eV). At still higher energies, there follows a number of weak features (D: 1576.8; E: 1580.0; F: 1582.3; G: 1587.8 eV) in a dampened series inside the XANES region (Bianconi 1988). Further wide, weak and yet evident undulations follow up-energy in the EXAFS region (not shown; cf. Wong et al. 1994)

The energies of the K-edge features do not change when quartz is used instead of YB_{66} (cf. Kinoshita et al. 1997). However, the spectrum obtained with the YB_{66} monochromator is definitively less intense than that obtained with quartz, as it could be expected by analogy from comparative results on the peak-reflectivity of beryl (Schaefers et al. 1992). Such a reduction distributes over the entire spectrum (Fig. 2a); a possible, minor difference is at pre-peak A', which is enhanced when quartz is used as monochromator, not to mention that a glitch occurs at ≈1594 eV in the spectrum obtained with YB_{66}. Therefore, despite having different reflectivities, the two monochromator crystals give spectra fully comparable and having the same resolutions; which of them is the best one is still an open question.

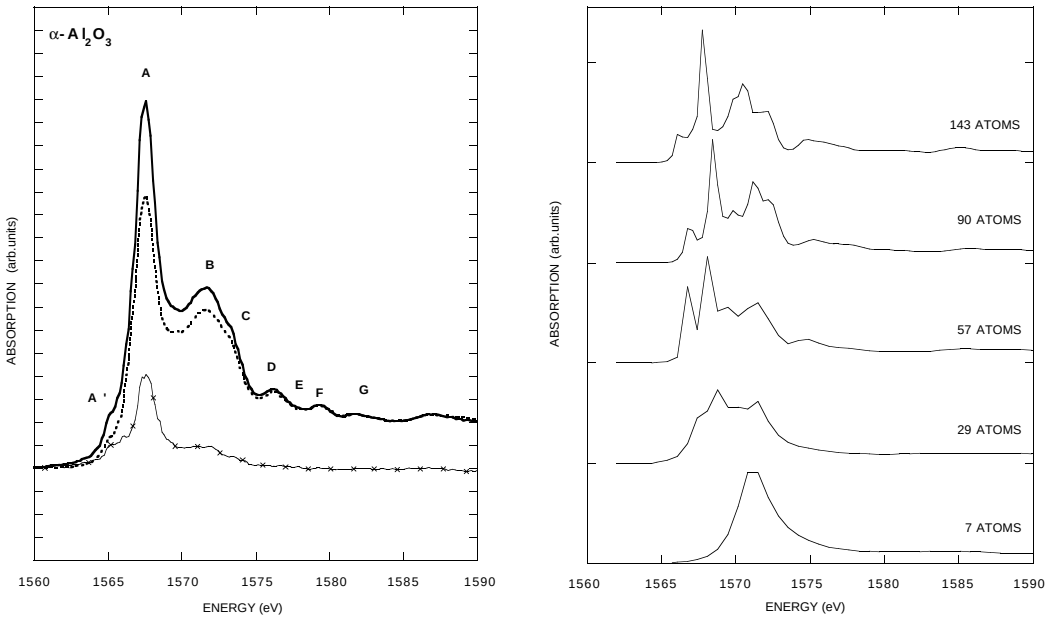

FIG. 2 – X-ray absorption spectra at the Al K-edge for pure synthetic α-Al_2O_3. Left panel: (**a**) experimental spectrum taken with quartz as monochromator (top), with YB_{66} (middle) and difference pattern between the two spectra (bottom); see text for explanation. Right panel: (**b**) Theoretical spectra computed for clusters of increasing numers of atoms and sizes.

Comparison of our α-Al_2O_3 experimental spectrum with those presented by other authors (Brytov et al. 1979; Wong et al. 1994; Ildefonse et al. 1994; Li et al. 1995, 1996; Cabaret et al. 1996; Kinoshita et al. 1997; note, however, that not all of them state whether their sample was

natural or synthetic) is satisfactory; when taken together, they allow a more accurate evaluation and a deeper discussion than it was possible before.

The overall appearance of the XANES spectra of artificial "corundums" COR 1 to COR 5 is always the same (Fig. 3), and is entirely consistent with the spectra of our reference α-Al_2O_3 and of natural corundum COR 6 (Fig. 3, bottom) taken under the same experimental conditions: all features are at the same energies (within $\pm 2\sigma$) as those recorded in the pure α-phase spectrum. Nevertheless, at a closer examination, subtle differences appear that subtraction methods enhance and make evident. The discussion that follows is based essentially on what arises from the application of these methods, as already commonly used in the analysis of x-ray dichroism results. Note that in all cases our spectra were first normalized to 1 well ahead from the edge, at 1585 eV; thus, the ticks in the ordinate scale of all figures are at constant 0.5 intervals, and the plotted results are rigorously comparable.

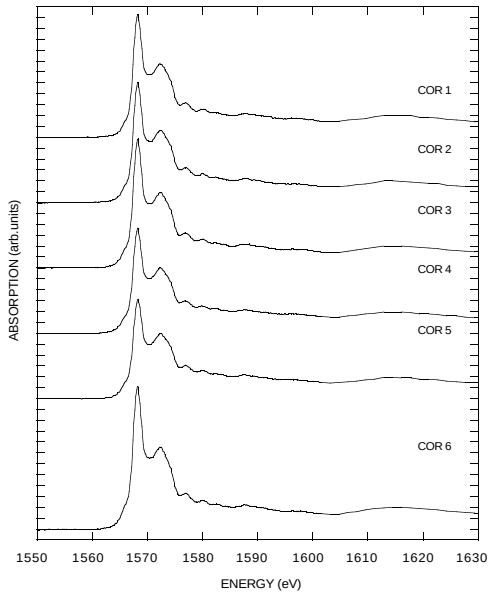

FIG. 3 – Experimental X-ray absorption spectra at the Al K-edge for synthetic "corundums" COR 1 to COR 5 and for natural "ruby/sapphire" corundum COR 6 (from top to bottom).

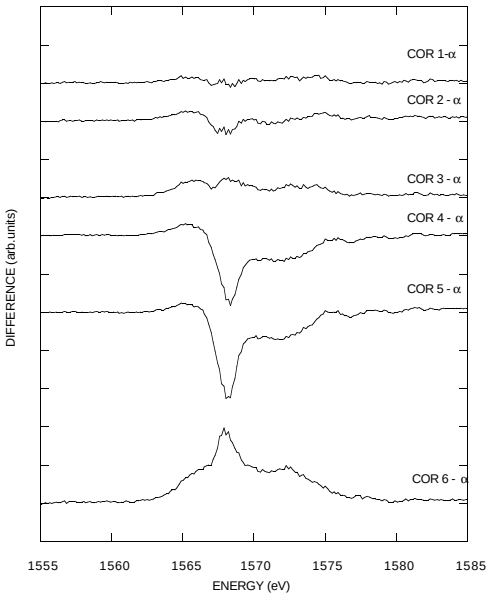

Fig. 4 - Difference spectra of synthetic and natural technical "corundums" *versus* pure synthetic α-Al_2O_3 (top to bottom, as in Fig. 3).

5 – DISCUSSION

The pure α-alumina experimental XANES spectrum can be easily reproduced by MS calculation, as shown already by Cabaret et al. (1996). The result of our independent calculation is given in Fig. 2b for a 143-atom (59 Al + 74 O) cluster, and the full sequence of the spectra computed for clusters containing an increasing number of atoms is given in Fig. 2 (right panel).

The very simplest cluster, which consists of the Al absorber and its 6 O nearest neighbors, generates a single, sharp peak with its maximum located at ~4.0 eV above the threshold. Adding atoms to this cluster (i.e., increasing its size) makes this sharp peak migrate toward lower energies and become broader; furthermore, it induces the formation of another peak, at first in the form of a shoulder on the higher energy side, then as a fairly well-resolved

feature that progressively migrates towards lower energies and increases in height. Only when the cluster contains 57 atoms (21 Al + 36 O) do other peaks appear, while the last-mentioned peak becomes so strong as to overcome the white-line. New peaks develop also in a cluster containing 90 atoms (41 Al + 49 O). As a matter of fact, with a cluster of this size the essential features of the final spectrum are attained, including the correct ratios in the height of the white-line relative to the peaks that follow. The correlation between experimental and calculated energy features is very good in the IMS and FMS regions, but it becomes poor in the first 5 eV from threshold, probably because of as yet unresolved problems with the average potentials which do not describe appropriately the real potentials. Clusters with further addition of atoms do not appear to ameliorate results; in fact, the appearence of new features not to be found in the experimental spectra suggests that new MS channels are being activated that are not real, and, by inference, that in the Al_2O_3 system the cluster probed by the emitted photoelectron is, at the Al K-edge energy, is of the order of 90-100 atoms. In fact, it is in the 90-atom cluster that the small pre-peak A' develops and becomes significant. This is in agreement with Cabaret et al. (1996 p. 3695), who consider pre-peak A' to be a signature of the medium-range internal order of corundum, and with our previous findings on garnet (Wu et al. 1996a). However, we do not agree with their assignment (which is also Brytov et al.'s 1979 p. 144 and Li et al.'s 1995 p. 435) that A' corresponds to dipole-forbidden transitions of Al 1*s* electrons to antibonding *s*-like states. We rather believe, as it turns out from our MS simulations which were carried out only by using dipole transitions, that A' is due to hybridization between Al *p*-orbitals and the empty *p*-orbitals of the outer O shells probed by photoelectrons in large clusters. We add, to confirm our interpretation, that pre-peak A' changes in height in technical "corundums", where it becomes sensitive to impurities. Therefore, the 90-atom cluster contains all information to unequivocally clarify that (i) white-line A is an essential atomic feature arising from short-range order, whereas (ii) all other small peaks in the spectrum, which closely match those recorded experimentally, are features that mark a medium- to long-range structural order i.e., they arise from interactions of the photo-electron with atoms in the second (or higher) coordination sphere (cf. Wu et al. 1996a).

However, when comparing our calculation with Cabaret et al's (1996), we note some differences which we explain with the different potentials used: in contrast to our Xα, Cabaret et al. (1996) made use of the Dirac-Hara exchange potential, which is less attractive and vanishes for high-energy.

To evaluate quantitatively the spectral differences among the investigated artificial samples, in Fig. 4 we report the difference spectra obtained by subtracting from the experimental XANES spectrum of each technical "corundum" (Fig. 3) that of our pure α-Al_2O_3 standard (Fig. 2). Three types of behavior can easily be detected:

1. A flat pattern: COR 1, COR 2, and COR 3 give no residuals, or just very small ones, and only in the energy region of the white-line; however, COR 3 residuals are always positive, whereas those given by COR 1 and COR 2 are both positive and negative on both sides of the zero line, and show a definite negative trend only at the white-line;
2. A flat pattern with fairly strong negative residuals over the entire FMS region: COR 4 and COR 5; it may be described as an amplification of the difference pattern given by COR 1 and COR 2;

3. A flat pattern with just as strong positive residuals, again over the entire FMS region: COR 6; this would be an amplification of the COR 3 case.

At a first sight, the difference pattern behaviors can be correlated to the bulk chemical compositions of the samples (Table I), the purest ones (COR 1 and COR 2) being the least different from pure α-alumina, and the impurest ones the most. However, this is contradicted by the residuals obtained when subtracting the α-spectrum from the COR 6 one.

Thus, we deemed it useful to perform a difference analysis of our technical "corundums" in relation to our natural "ruby/sapphire" COR 6 (Fig. 5).

All synthetic samples display the same pattern of negative deviation from the natural sample, and all these deviations are significant. Deviations concentrate again in the K-edge region, being greatest at the white-line (A) and for sample COR 5, and decrease in the order COR 5 -> COR 4 -> COR 2 -> COR 1 -> COR 3 i.e., in the same order as the total contents of chemical impurities, but for COR 3 (Table I).

According to Fig. 5, our technical "corundums" may again be distinguished in two groups: (a) COR 1, COR 2 and COR 3 from one side, and (b) COR 4 and COR 5 from the other side

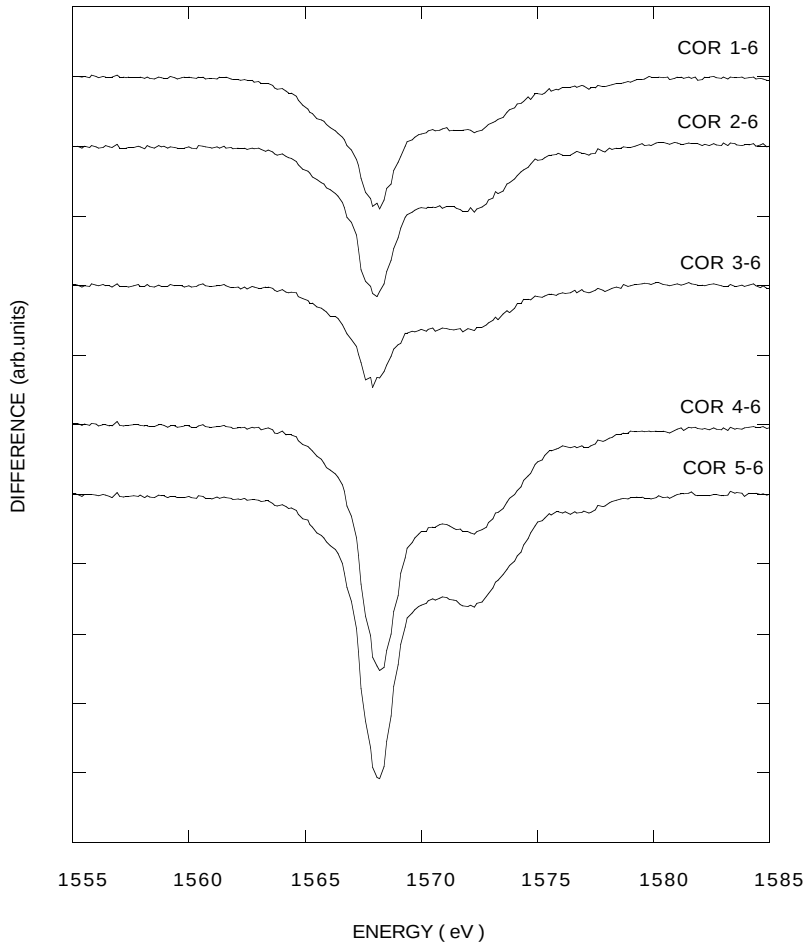

FIG. 5 – Difference spectra of synthetic technical "corundums" *versus* natural "ruby/sapphire" corundum COR 6 (top to bottom, as in Fig. 3).

In group (a), differences concentrate on features A and B (note COR 3, in particular) and, in addition, possibly, on A' for COR 1. In group (b) the difference patterns are very well-structured in both the FMS and IMS regions, and practically mimic negatively the entire XANES spectrum; in other words, they are distributed evenly over it, just as it occurred when we were comparing the same sample of the α-phase taken by using two different monochromator crystals (Fig. 2a, bottom). We interpret the observed behaviors in the sense that the factor provoking the observed difference interests the entire corundum structure in group (b) i.e., that there is a medium- to long-range order distribution of the factor causing these differences over the entire crystal. By contrast, for group (a) we argue for a factor affecting mainly the white-line i.e., anything related only to the first-coordination sphere (short-range-order).

Turning now to chemical and physical evidence, what mainly discriminates COR 6 from group (b) samples (COR 4 and COR 5) is chemical composition i.e., the total number of substitutional defects distributed over the entire corundum structure; however, these defects cannot affect substantially the Al K-edge spectrum since Al is almost entirely in the α-phase (see above). To further support this interpretation: "ruby/sapphire" COR 6 is very impure, chemically as well as physically; yet it gives a structured difference pattern with well-enhanced B and C features as well as with several minor features up-energy. Our implication is that most atoms other than Al that were detected and measured in the bulk sample are tied in the physical impurities, and only minor amounts of them enter the α-phase, although being still in an amount large enough so as to contribute to its blue and red colors (Schmetzer & Bank 1981). XANES therefore confirms the XRD data of Table II.

By contrast, group (a) samples (COR 1, COR 2 and COR 3) differ from COR 6 not only in their chemistries, but for containing admixed "β-alumina" (see above), a phase where only a portion of Al (2 atoms out of 3) is indeed in the octahedral coordination (as in the α-phase), whilst another portion of it (1:3) is in the tetrahedral coordination (Edström et al. 1991).

Therefore, it seems to be a obvious conclusion that the observed differences, albeit all negative, are related to two different factors: (i) reduced amount of Al in the samples for group (b), the coordination and structure of Al in "corundum" however being the same; and (ii) reduced amount of octahedral Al for group (a), in spite of the fact that the total amount of Al in the bulk samples is even greater, and owing to the fact that one third of it is displaced from the octahedral site to the tetrahedral one.

In aluminosilicates, the Al K-edge is well-known to undergo a significant negative shift (2.2~5.2 eV) when the Al coordination number lowers from 6 to 4 (McKeown et al. 1985; Wong et al. 1994; Li et al. 1995; Cabaret et al. 1996; Wu et al. 1997; Mottana et al. 1997). In our Fig. 5 this shift probably explains the change of slope observed at lower energy for the COR 1 and COR 2 patterns, which could be misunderstood for a pre-peak while is to be referred to the tetrahedral Al present in the admixed β-phase.

When now comparing samples inside each group, we confirm that the very minor differences existing between COR 1 and COR 2 viz. COR 3 (Fig. 6, top) appear to be such as not to be quantitatively significant at all. Yet, some little difference arises because of the changes in the sign of the residuals: they are positive for COR 1 minus COR 2, and always negative when COR 3 is taken into consideration. Since samples COR 1, COR 2 and COR 3 are all very

pure in composition (≈99 wt.% Al_2O_3) and differ only for their contents of $NaAl_{11}O_{17}$, the "β–alumina" phase (≈10 vol.% in COR 1, but only ≈3~5 vol.% in COR 2 and COR 3, the latter however being richer in Cr_2O_3; see above), we explain the pattern difference in the sense that large differences in the amounts of admixed "β-alumina" do not affect substantially the Al K-edge spectra, but, when the "β-alumina" amounts are nearly the same, the effect of the chemical impurities present in either the α- or the β-phase becomes significant. However, a check at Table I shows that the different behavior of COR 2 to COR 3 depends on Ti, rather than on Cr (as believed).

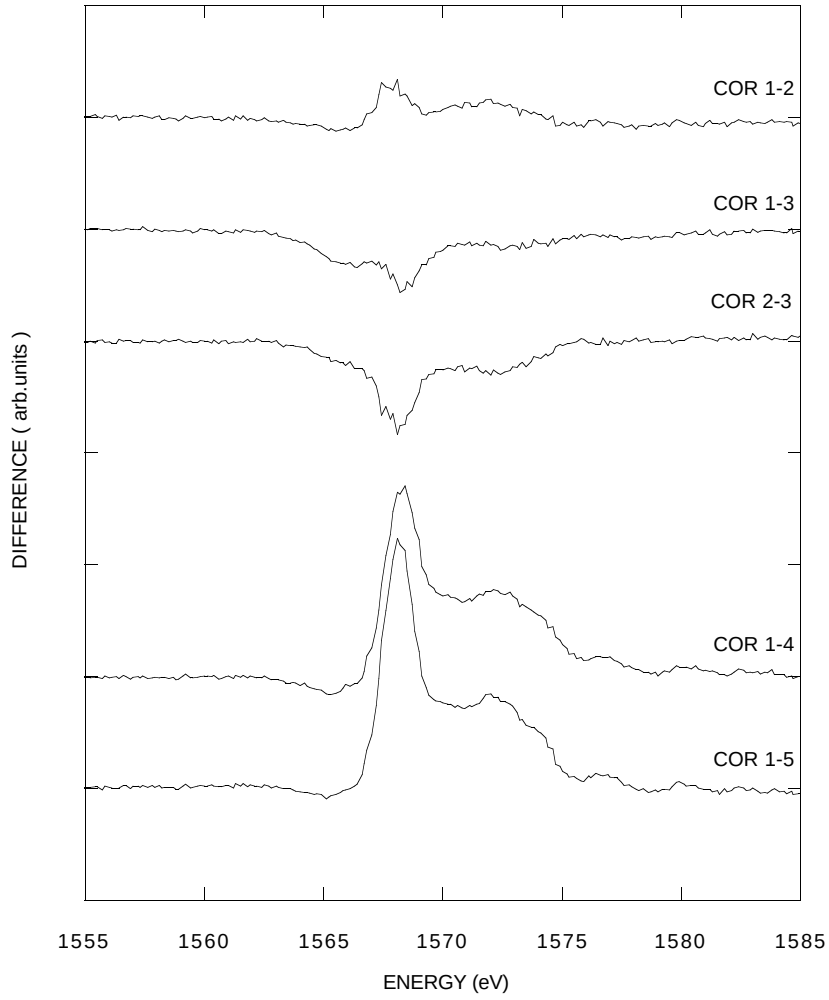

FIG. 6 – Difference spectra of technical "corundums": (a) COR 1 vs. COR 2 and COR 3; (b) COR 2 vs. COR 3; (c) COR 1 vs. COR 4 and COR 5.

We stress as a major experimental conclusion the fact that the COR 2 vs. COR 3 difference pattern shows an unexpected relationship with the Al K-edge XANES spectrum; this implies that the absorption of Al K X-rays by "precious pink special corundum" COR 3 is directly affected by the presence of Ti; in other words, that this element is not present as a random impurity, but it regularly substitutes for Al in the α-alumina lattice: it follows that

omissional defects must be present to compensate for the difference in valence electrons.

Following the same line of reasoning, the significant differences existing between COR 1 and group (b) samples (COR 4 and COR 5), which also follow a regular pattern rather similar to an absorption spectrum with its maximum at white-line A and with undulations at higher energy, make it reasonable to suggest that some relationships exists with the structural state of these materials.

Samples COR 4 and 5 are both considerably less pure in their bulk (≈97 wt.% Al_2O_3) than the previous ones and, in particular, have rather high contents of transition metals (Fe, Ti, Zr), Mg and Si. However, XRD confirms the presence in them of physical impurities of titanates, spinels etc., so that we can believe all the chemical impurities to be bound in them, and interpret the observed structured difference pattern for Al to reflect the high purity of the α-phases, in other words, COR 1 and COR 2 contain two types of Al (in octahedral coordination in the α- and β-phases, and in tetrahedral coordination in the β-phase), so that the Al absorption for $^{[6]}$Al is comparatively reduced; COR 4 and COR 5 contain only the α-phase and this is almost free from substitutions: their Al cross section is greater than those of the other samples.

6 – CONCLUSION

Experimental spectra of five artificial “corundums” synthesized for technical purposes, as well as of one natural “ruby/sapphire” corundum prepared as a geochemical standard, can be explained in terms of the defect structures of the materials, once the electronic properties of pure α-phase alumina (corundum) are clarified by means of theoretical spectra calculated *via* the multiple-scattering formalism.

It appears that most differences in the experimental spectra reflect the degree of incorporation of foreign atoms in the α-alumina lattice. In particular, technical “corundums” which, from the “bulk-chemical” standpoint, appear to be the most impure, in fact contain the purest α-phases, while those chemically purest, but containing “β-alumina” as an admixed physical impurity, have their Al K-edge XANES pattern sensibly affected. However, differences are not strictly related only to bulk compositions: certain α-phase technical “corundums” differ from pure synthetic α-alumina because they incorporate foreign atoms (mainly Ti) substituting for Al; others because their degrees of short-range order are different; and still others because there are differences in their medium- to long-range order.

Thus XANES, when carefully evaluated in an appropriate chemical and structural system i.e., under favorable conditions like the present ones, proves a reliable method for testing the electronic properties and the local structures of samples where minor amounts of the absorber atom are being interfered *viz*. substituted by dilute atoms of various different types.

7 – ACKNOWLEDGEMENTS

Work performed at UVSOR thanks to support within proposal No. 6-D-567 and contributions of a UE HC&M project under contract 94-0551, and of CNR under project 95.00303.CT05.

Dedicated to C.T. Prewitt in the occasion of his 65th birthday.

REFERENCES

Balzarotti, A. & Bianconi, A. (1976) Electronic structure of aluminum oxide as determined by x-ray photoemission. Physica Status Solidi B 76, 689-694.

Batra, I.P. (1981) Electronic structure of α-Al_2O_3. Journal de Physique C: Solid State Physics 15, 5399-5410.

Benfatto, M. & Natoli, C.R. (1986) Unified scheme of interpretation of the x-ray absorption spectra based on the multiple scattering formalism. Italian Physical Society Conference Proceedings 5, 59-62.

Bianconi, A. (1988) XANES spectroscopy. In: D.C. Konigsberger & Prins, Eds. X-ray absorption: principles, applications, techniques of EXAFS, SEXAFS and XANES. p. 573-662. Wiley, New York.

Blonski, S. & Garofalini, S.H. (1993) Molecular dynamics simulations of α-alumina and γ-alumina surfaces. Surface Science 195, 163-174.

Brytov, I.A., Konashenok, K.I. & Romashchenko, Yu.N. (1981) Crystallochemical effects of Al K and Si K emission and absorption spectra for silicate and aluminosilicate minerals. Geochemistry International 16, 141-154.

Cabaret, D., Sainctavit, P., Ildefonse, P. & Flanck, A.-M. (1996) Full multiple-scattering calculations on silicates and oxides at the Al K edge. Journal de Physique: Condensed Matter 8, 3691-3704.

Causa', M., Dovesi, R., Roetti, C., Kotomin, E. & Saunders, V.R. (1987) A periodic ab initio Hartree-Fock calculation on corundum. Chemical Physics Letters 140, 110-113.

Ciraci, S. & Batra, I.P. (1983) Electronic structure of α-alumina and its defect states. Physical Review B 18, 981-991.

Clementi, E. & Roetti, C. (1974) Atomic data and nuclear data tables. Vol. 14, No. 3-4. New York: Academic Press.

Edström, K., Thomas, J.O. & Farrington, G.C. (1991) Sodium-ion distribution in Na^+ β-alumina: a crystallographic challenge. Acta Crystallographica B 47, 210-216.

Hamilton, D.L. & Henderson, M.B. (1968) The preparation of silicate compositions by a gelling method. Mineralogical Magazine 36, 832-838.

Ildefonse, Ph., Kirckpatrick, R.J., Montez, B., Calas, G., Flank, A.M. & Lagarde, P. (1994) ^{27}Al MAS NMR and aluminum x-ray absorption near edge structure study of imogolite and allophanes. Clays and Clay Minerals 41, 176-187.

Kinoshita, T., Takata, Y., Matsukawa, T., Aritani, H., Matsuo, S., Yamamoto, T., Takahashi, M., Yoshida, H., Yoshida, T. & Kitajima, Y. (1997) Performance of YB_{66} soft X-ray monochromator crystal at the wiggler beamline of UVSOR facility. UVSOR Activity Report 1996, 198-199.

Kirfel, A. & Eichhorn, K. (1990) Accurate structure analysis with synchrotron radiation. The electron density in Al_2O_3 and Cu_2O. Acta Crystallographica A 46, 271-284.

Li, D., Bancroft, G.M., Fleet, M.E., Feng, X.H. & Pan, Y. (1995) Al K-edge XANES spectra of aluminosilicate minerals. American Mineralogist 80, 431-440.

Li, D., Bancroft, G.M. & Fleet, M.E. (1996) Coordination and local structure of Si and Al in silicate glasses: Si and Al K-edge XANES spectroscopy. In: "Mineral Spectroscopy: A Tribute to Roger G. Burns" (M.D. Dyar, C. McCammon & M.W. Schaefer, eds.). Geochemical Society Special Publication No. 5, 153-163.

Mattheiss, L. (1964) Energy bands for the iron transition series. Physical Review A 134, 970.

McKeown, D.A. (1989) Aluminum x-ray absorption near-edge spectra of some oxide minerals: calculation versus experimental data. Physics and Chemistry of Minerals 16, 678-683.

McKeown, D.A., Waychunas, G.A., & Brown, G.E. Jr (1985) EXAFS study of the coordination environment of aluminum in a series of silica-rich glasses and selected minerals within the Na_2O-Al_2O_3-SiO_2 system. Journal of Non-Crystalline Solids 74, 349-371.

Mottana, A., Murata, T., Wu, Z.Y., Marcelli, A. & Paris, E. (1996) The local structure of Ca-Na pyroxenes. I. XANES study at the Na K-edge. Physics and Chemistry of Minerals 24, 500-509.

Mottana, A., Robert, J.-L., Marcelli, A., Giuli, G., Della Ventura, G., Paris, E. & Wu, Z.Y. (1997) Octahedral versus tetrahedral coordination of Al in synthetic micas determined by XANES. American Mineralogist 82, 497-502.

Murata, T., Matsukawa, T., Naoe', S., Horigome, T., Matsudo, O. & Watanabe, M. (1992) Soft x-ray beamline BL7A at the UVSOR. Review Science Instruments 63, 1309-1312.

Natoli, C.R., Benfatto, M., Brouder, C., Ruiz Lopez, M.Z. & Foulis, D.L. (1990) Multichannel multiple-scattering theory with general potentials. Physical Review B 42, 1944-1968.

Newnham, R.E. & deHaan, Y.M. (1961) Refinement of the α-Al_2O_3, Ti_2O_3, V_2O_3 and Cr_2O_3 structures. Zeitschrift für Kristallographie 117, 135-137.

Norman, J.G. (1974) SCF-Xα scattered wave calculation of the electronic structure of $Pt(PH_3)_2O_2$. Molecular Physics 81, 1191.

Peters, C.R., Bettman, M., Moore, J.W. & Glick, M.D. (1971) Refinement of the structure of sodium β-alumina. Acta Crystallographica B 27, 1826-1834.

Rocca, F., Kuzmin, A., Purans, J. & Mariotto, G. (1996) X-ray-absorption spectroscopy of Nd^{3+}-exchanged β-alumina crystal. Physical Review B 53, 11444-11450.

Schaefers, F., Müller, B.R., Wong, J., Tanaka, T. & Kamimura, Y. (1992) YB_{66}: a new soft X-ray monochromator crystal. Synchrotron Radiation News 5[2], 28-30.

Schmetzer, K. & Bank, H. (1981) The color of natural corundum. Neues Jahrbuch für Mineralogie Monatshefte [1981], 59-68.

Slater, J.C. (1979) The self-consistent field for molecules and solids. In: Quantum theory of molecules and solids. McGraw Hill, New York.

Sousa, C., Illas, F. & Pacchioni, G. (1993) Can corundum be described as an ionic oxide? Journal of Chemistry and Physics 99, 6818-6823

Tessadri, R. (1996) Corundum materials COR 1 to COR 6: six new candidates for chemical characterization as "industrial-mineralogical" standard reference materials. Mitteilungen der Österreichischen Mineralogischen Gesellschaft 141, 130-131.

Tossel, J.A. (1975) The electronic structures of Mg, Al and Si in octahedral coordination with oxygen from SCF Xα calculations. Journal of Chemistry and Physics of Solids 36, 1173-1180.

Tyson, T.A., Hodgson, K.O., Natoli, C.R. & Benfatto, M.(1992) General multiple-scattering scheme for the computation and interpretation of x-ray absorption fine structure in atomic clusters with applications to SF_6, $GeCl_4$ and Br_2 molecules. Physical Review B, 46, 5997-6019.

Watanabe M (1991) UVSOR at IMS. Synchrotron Radiation News 4 [3]: 12-17.

Wong, J., George, G.N., Pickering, I.J., Rek, Z.U., Rowen, M., Tanaka, T., Via, G.H., DeVries, B., Vaughan, D.E.W. & Brown, G.E. Jr. (1994) New opportunities in XAFS investigation in the 1-2 keV region. Solid State Communications 91, 559-561.

Wu, Z.Y., Marcelli, A., Mottana, A., Giuli, G., Paris, E. & Seifert, F. (1996a) Effects of higher-coordination shells in garnets detected by x-ray-absorption spectroscopy at the Al *K* edge. Physical Review B 54, 2976-2979.

Wu, Z.Y., Mottana, A., Marcelli, A., Natoli, C.R. & Paris, E. (1996b) Theoretical analysis of X-ray absorption near-edge structure in forsterite, Mg_2SiO_4-Pbnm, and fayalite, Fe_2SiO_4-Pbnm, at room temperature and extreme conditions. Physics and Chemistry of Minerals 23, 193-204.

Wu, Z.Y., Marcelli, A., Mottana, A., Giuli, G. & Paris, E. (1997) Al coordination and local structure in minerals: XAFS determinations and multiple-scattering calculations for K-feldspars. Europhysics Letters 38, 465-470.